International Journal of Biological Macromolecules 86 (2016) 80–88

Contents lists available at ScienceDirect

International Journal of Biological Macromolecules

journal homepage: www.elsevier.com/locate/ijbiomac

Combination of lignin and L-lactide towards grafted copolymers from lignocellulosic butanol residue

Enmin Zong[a,*], Jinhua jiang[a], Xiaohuan Liu[b,c,*], Shenyuan Fu[b], Yuzhi Xu[c], Fuxiang Chu[c]

[a] Zhejiang Provincial Key Laboratory of Plant Evolutionary Ecology and Conservation, Taizhou University, Taizhou 318000, PR China
[b] School of Engineering, and National Engineering and Technology Research Center of Wood-based Resources Comprehensive Utilization, Zhejiang Agriculture and Forestry University, Hangzhou Lin'an 311300, PR China
[c] Institute of Chemical Industry of Forestry Products, CAF, Nanjing 210037, PR China

ARTICLE INFO

Article history:
Received 9 September 2015
Received in revised form 10 January 2016
Accepted 11 January 2016
Available online 14 January 2016

Keywords:
Lignocellulosic butanol residue
Ring-opening polymerization (ROP)
Graft copolymer
L-Lactide
UV absorption

ABSTRACT

A series of BBL-*graft*-poly (L-lactide) copolymers were synthesized via ring-opening polymerization (ROP) of L-lactide (L-LA) with a biobutanol lignin (BBL) initiator and a triazabicyclodecene (TBD) catalyst under free-solvent at 135 °C. By manipulating the mass ratio of BBL/LLA, BBL-*g*-PLLA copolymers with tunable number–average molecular weight (M_n) (2544–7033 g mol^{-1}) were obtained. The chemical structure of PLLA chains was identifiable by FT-IR, ^{1}H NMR and ^{13}C NMR spectroscopies, in combination with UV–vis spectra to provide support for the existence of the BBL in the copolymer. This provided solid evidence for the successful synthesis of BBL-*g*-PLLA copolymer. The thermal properties and surface characterization of BBL-*g*-PLLA copolymers were different from those of linear PLLA. Furthermore, the BBL-*g*-PLLA copolymer film showed good absorption capacity in the UV region and high transparency in the visible light region, which was expected to find significant applications in UV-protective coating film.

1. Introduction

As the second most abundant organic compound in nature after cellulose, lignin has received an increasing attention over the last decade because of the rapid consumption of petroleum and petro-chemicals [1]. Lignin shows a highly branched and irregular macromolecular structure, depending on the biomass species, growing conditions and extraction procedures [2–4]. Lignin is made up of three different types of phenylpropanoid monomers such as p-coumaryl, coniferyl and sinapyl alcohols and linked by aryl-ether, alkyl-ether, and carbon–carbon covalent bonds into a highly branched polymer network [5]. Currently, lignin is being utilized as a low-grade boiler fuel to provide heat from the combustion, or be disposed as waste [6]. Furthermore, hydrogen bonding and van der waals interactions led to aggregation of lignin, resulting in poor compatibility with other materials [7]. Butanol, an important industrial chemical, is considered as a superior liquid fuel with a potential to substitute for fossil fuel [8]. It is noted that lignocellulosic biomass can be used to produce butanol from biorefinery processes based on corn and wheat straw [9], which brings a large amount of lignocellulosic butanol residue, called biobutanol lignin (BBL). There is no doubt that the development of a way to convert BBL to the higher-valued products could help to boost the economic viability of the biobutanol industries. Consequently, the conversion of BBL to higher-valued materials is an active area of research [9–13].

Due to the hydroxyl groups, lignin is most often functionalized by esterification [14,15]. Although this method could improve the compatibility between lignin and blended polymeric materials, it has limited impact on changing lignin toward desirable properties [16]. Graft polymerization is an attractive approach to modify the lignin, resulting in lignin graft copolymers used for a much wider range of applications [17]. In order to obtain the lignin graft copolymers, there are two general strategies: the so-called "grafting from" approach, where polymer chains are built on the lignin cores, and the "grafting onto" approach, where polymer strands are synthesized firstly and subsequently grafted to the lignin cores [18]. Among the graft polymerization methods, the "grafting from" technology is the most usually used procedure which can produce high graft density of copolymer compared to the "grafting onto" route [19]. Currently, using the "grafting from" route to produce lignin graft copolymers mainly includes two types of polymerization reactions. The first one is the ring opening polymerization (ROP), which uses surface hydroxyl groups of lignin as the initiator, while the second one is that firstly requires the creation of lignin "macro"-radical, and then initiates the polymerization of other vinylic monomers [20].

* Corresponding authors.
E-mail addresses: zongenmin@163.com (E. Zong), liuxiaohuancaf@163.com (X. Liu).

http://dx.doi.org/10.1016/j.ijbiomac.2016.01.043
0141-8130/

Presently, there is a great interest in biomaterials from renewable resources due to low-cost, biodegradability and biocompatibility [21]. Increasing attention has been paid to obtain biomaterials from lactones and lactides. Currently, PLA is the most commonly biodegradable polymers and produce from Lactic acid (LA). However, there are some undesirable attributes of PLA such as its high cost, brittleness, poor UV light barrier properties and poor thermal stability, which have limited replace for commercial polymeric materials [22]. Overcoming aforementioned disadvantages, the grafting copolymerization of BBL with L-lactide is a promising approach, which can decrease the cost and improve thermal resistance and UV absorption capacity of PLLA [12,22].

Ring-opening polymerization (ROP) is considered to be an effective "graft from" polymerization technique for the preparation of lignin graft PLLA copolymers. The multiple hydroxyl groups at the surface of lignin could be act as available reactive sites for ROP [23,24]. Preparation of polyesters from lactones via ROP is the most conventional synthesis route at present. It is carried out in melt or in solution by different polymerization mechanisms (e.g., anionic, cationic, coordination-insertion), which depend on the used catalyst. Little metal residues will be in the final products when using metal-based catalysts, resulting in restricting the application in packaging [25]. Herein, the syntheses of BBL-*g*-PLLA copolymers in this study were performed using triazabicyclodecene (TBD) as the organic catalyst. Furthermore, TBD has been proven to be an effective catalyst for ROP of LLA in some literatures [22,25,26].

Recently, we have successfully prepared some different lignin graft copolymers using BBL as raw materials [10–13]. It was worth noting that BBL possessed high chemical activity [9], in comparison with kraft lignin or lignosulfonate studied in the literatures. This was because the biochemical reaction process of biomass was performed under moderate reaction condition, and some chemical groups (e.g., phenolic hydroxyl and alcoholic hydroxyl) were well preserved [27], In this paper, as a novel type of lignin, BBL was modified by LLA through "grafting from" ROP to combine the properties of BBL and PLLA, which could be viewed as a continuation of the abovementioned work, and BBL-*graft*-PLLA copolymer was synthesized via a practical route (Scheme 1), that is, "Grafting from" ROP was carried out to prepare a series of BBL-*graft*-PLLA copolymers using TBD as catalyst under solvent-free conditions. The graft copolymer was fully characterized by FT-IR, NMR, UV–vis, GPC, TGA, DSC, XPS, and FE-SEM. Furthermore, the UV absorption capability of the BBL-*g*-PLLA coating film was also explored in this study. The long term of this work is to fully utilize lignocellulosic butanol residue as the raw material to produce the biopolymer which can be used as UV-absorbent film.

2. Experimental section

2.1. Materials

Lignocellulosic butanol residue used in this work was supplied by songyuan bairui bio-polyos Co., Ltd., from Jilin province (China) and used before purified as described in previous report [11]. The physical and chemical characteristics of this biobutanol lignin (BBL) had been reported in our earlier work (details for Table 1) [10]. The L-lactide (L-LA) (optical purities, 99.5%) was purchased from Changchun SinoBiomaterials Co., Ltd., and used as received. 1, 5, 7-triazabicyclo [4.4.0] dec-5-ene (TBD, 98%) was obtained from Sigma–Aldrich and used as received. Acetic acid, dichloromethane and anhydrous methanol were of analytical reagent grade and used without further purification.

2.2. Typical polymerization procedure (Table 2, BBL-PLLA-5%)

As shown in Scheme 1, the synthesis procedure of BBL-*g*-PLLA copolymer was described as follows [22]. The suitable amount of

Table 1
Chemical composition and structural properties of biobutanol lignin (BBL).

BBL		
	C [wt.%]	62.7
	H [wt.%]	5.47
	O [wt.%]	31.96
	N [wt.%]	0.75
	S [wt.%]	0.12
	C_9 formula	$C_9H_{8.160}O_{2.996}N_{0.094}S_{0.0\,06}(OCH_3)_{0.594}$
^{1}H NMR analysis	Phenolic-OH [mol g^{-1}]	2.95
	Aliphatic-OH [mol g^{-1}]	2.67
	Methoxyl [mol g^{-1}]	3.24
GPC analysis	M_w [g mol^{-1}]	876
	M_n [g mol^{-1}]	543
	PDI	1.61

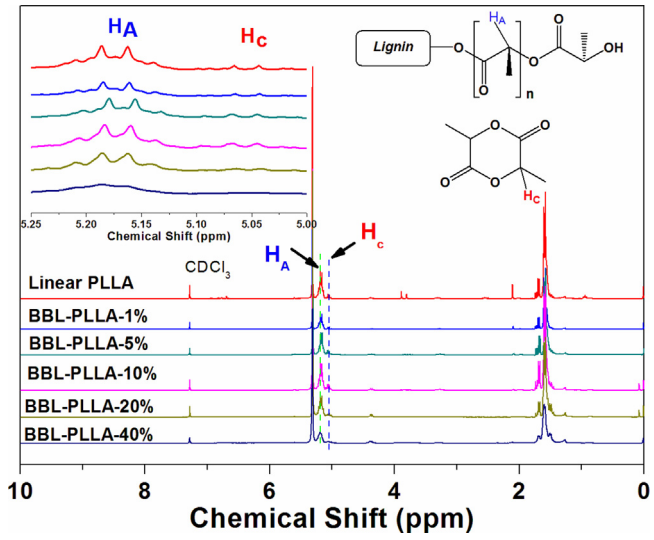

Fig. 1. ^{1}H NMR spectra for calculation of the conversion of LLA.

BBL (0.5 g, 5 wt.%), LLA (9.5 g, 95 wt.%) and TBD (1.5 g, 1.5 wt.%) were mixed in a polymerization reactor under magnetic stirring and heated in an oil bath to 135 °C for 4 h in a nitrogen atmosphere. After the polymerization reaction finished, the reactor medium was finally cooled to room temperature. The resulting black product was dissolved in a mixture solution of dichloromethane and acetic acid. When the residue dissolved, the sample was withdrawn from the flash with degassed syringes to determine the LLA conversion by ^{1}H NMR analysis in $CDCl_3$. The conversion of LLA was calculated using the following Formula (1), according to the integration of the L-lactide methide signal (H_c, 5.03 ppm) against the integration of PLA methide signal (H_a, 5.16 ppm) in ^{1}H NMR spectra of samples (Fig. 1).

$$C(\%) = \frac{H_a}{H_a + H_c} \times 100\% \quad (1)$$

Finally, the remainder of the crude reaction mixture was precipitated with methanol to obtain a solid precipitate, and collected by centrifugation. The produced BBL-PLLA-5% copolymer was isolated and dried in vacuum at 50 °C for 12 h. The syntheses of the rest of BBL-*g*-PLLA copolymers were similar to the procedure described above. To better understand the changes suffered by BBL as a result of the chemical reaction, a blank sample was prepared (linear PLLA). The linear PLLA polymer was obtained under the same reaction conditions, but instead using TBD (75 mg, 0.539 mmol) together with 2-methoxy-4-propylphenol (232 mg, 1.396 mmol) as initiator for the polymerization of LLA (5 g, 34.7 mmol). The linear PLLA sample

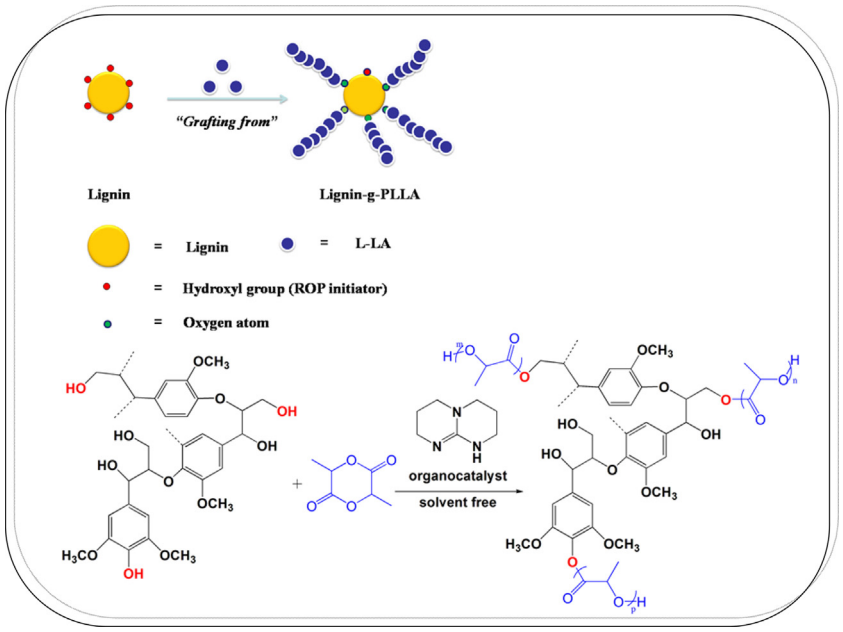

Scheme1. Synthesis of BBL grafted PLLA copolymers by a "grafting from" strategy.

Table 2
Reaction conditions and results for the preparation of grafted copolymers[a].

Sample Code[b]	Content [wt.%]		Conv.[c] [%]	Mw [g mol^{-1}] GPC	Mn [g mol^{-1}] GPC	M_w/M_n[d]
	Raw materials					
	BBL	LLA				
Linear PLLA[e]	–	–	91.9	6424	3990	1.61
BBL-PLLA-1%	1	99	92.1	11213	7033	1.59
BBL-PLLA-5%	5	95	85.2	9504	6361	1.49
BBL-PLLA-10%	10	90	83.2	8778	5243	1.67
BBL-PLLA-20%	20	80	85.5	6074	2544	2.39
BBL-PLLA-40%	40	60	85.2		–	–

[a] Reaction were conducted at 135 °C for 4 h.
[b] Sample codes are defined as follows: the number behind "BBL-PLLA" stands for the mass content of BBL before the reaction.
[c] Determined by ^{1}H NMR (Fig. 1).
[d] Determined from the GPC analysis with polystyrene standards (Fig. 2).
[e] The linear PLLA was prepared as described in the experimental section, but instead using TBD (75 mg, 0.539 mmol) together with 2-methoxy-4-propylphenol (232 mg, 1.396 mmol) as initiator for the polymerization of LLA (5 g, 34.7 mmol).

was characterized using the same techniques as that used for BBL-*g*-PLLA copolymer samples. The details of BBL-*g*-PLLA copolymers and linear PLLA were summarized in Table 2.

2.3. Fourier transform infrared spectroscopy (FT-IR)

Attenuated total reflectance Fourier transform infrared (ATR-FTIR) spectrum of BBL-*g*-PLLA sample was recorded using a Nicolet (USA) IS10 instrument at room temperature in the wavenumber range of 600–4000 cm^{-1}.

2.4. Nuclear magnetic resonance spectroscopy (NMR)

^{13}C NMR and ^{1}H NMR spectrum were obtained at 298 K on a Bruker Avance 500 MHz spectrometer using tetramethylsilane as an internal standard. Each BBL-*g*-PLLA copolymer sample was dissolved in deuterated chloroform ($CDCl_3$) in sample tube.

2.5. Differential scanning calorimetry (DSC)

Glass transition temperatures (T_g) of BBL-*g*-PLLA copolymer and Linear PLLA samples were measured using a TA Instruments. The sample was weighed about 4–6 mg and placed into standard aluminum pans individually. The temperature was increased at a rate of 20 °C min^{-1}. T_g was determined from the second heating scan, and the first scan allowed us to discard thermal history of the sample.

2.6. Thermogravimetric analysis (TGA)

All thermogravimetric analysis were carried out on a TGA Q500 apparatus (TA instruments) ranging from 30 to 800 °C at a heating rate of 10 °C min^{-1} under a nitrogen flow rate of 100 mL min^{-1}.

2.7. Gel permeation chromatography (GPC)

All samples were allowed for dissolution in HPLC grade tetrahydrofuran (THF) for gel permeation chromatography (GPC) analysis. Sample concentrations were 1.0–5.0 mg mL^{-1}. The samples were filtered through polytetrafluorethylene (PTFE) membranes with a pore size of 0.45 μm prior to injection, and then a total of 100–150 μL of sample was injected.

2.8. Field-emission scanning electron microscopy (FE-SEM)

The morphologies of BBL and BBL-*g*-PLLA copolymer surface layers were investigated using a Hitachi S-4800 field-emission scanning electron microscopy (FE-SEM) at an accelerating voltage of 15 kV. The samples were sputter-coated with gold prior to SEM observation.

2.9. Water contact angle measurements

The contact angles of water droplets delivered from a needle connected to a syringe pump and deposited on the surface of the coating films which were obtained by drop-casting THF solutions of BBL-*g*-PLLA copolymer and drop-casting DMF solutions of BBL. The measurements were performed on a DSA100 (KRUSS, Germany) instrument. The averages of at least five contact angles for each substrate are reported.

2.10. X-ray photoelectron spectroscopy (XPS)

The chemical compositions of BBL and BBL-*g*-PLLA copolymer were determined using X-ray photoelectron spectroscopy (XPS). The measurements were carried out on a PHI 5000 Versa Probe XPS spectrometer (ESCALAB 250 US Thermo Electron Co). All spectra were calibrated to the binding energies of the C 1s peak at 284.6 eV binding energy controlled by means of the well-known photoelectron peaks of metallic Cu, Ag, and Au. The characteristic X-rays focus on C and O in this study.

2.11. UV Spectrophotometer

The optical properties of neat PLLA and BBL-*g*-PLLA coating films were carried out on a UV–vis Spectrophotometer (MAPADA UV-1800PC) in double-beam mode. The spectra were acquired using cleaned quartz slide as a reference while the wavelength region was between 200 and 800 nm.

3. Results and discussion

3.1. The characterizations and properties of BBL

According to the previous study of characterizations of BBL which were obtained by Hydrogen Nuclear magnetic resonance spectroscopy (^{1}H NMR) and Gel permeation chromatography (GPC) based on acetylated BBL, the main results are list in Table 1. BBL showed a high hydroxyl content of 5.62 mmoL g^{-1} (including 2.95 mmoL g^{-1} phenolic-hydroxyl and 2.67 mmoL g^{-1} aliphatic-hydroxyl). These data constituted a key point in this work because the surface of hydroxyl groups in lignin would be functionalized [24]. Moreover, the number average molecular weight (M_n) and polydispersity (PDI) of BBL was 543 g mol^{-1} and 1.61, respectively. It was worth noting that the PDI of BBL was low compared to Kraft or lignosulfonate lignin [28], which allowed assessing that this novel type of lignin possessed a lower polydispersity and a more defined structure [24].

3.2. Grafting of PLLA from BBL via ring-opening polymerization (ROP)

The synthesis is illustrated in Scheme 1. Starlike copolymers with a stiff lignin backbone and PLLA side chains were synthesized by the ring-opening polymerization (ROP) in the presence of triazabicyclodecene (TBD) as a catalyst under free-solvent. To obtain different number-average molecular weight (M_n) of BBL-*g*-PLLA copolymers, we had prepared a series of PLLA grafted BBL copolymers with BBL content varying from 1% to 40 wt.%

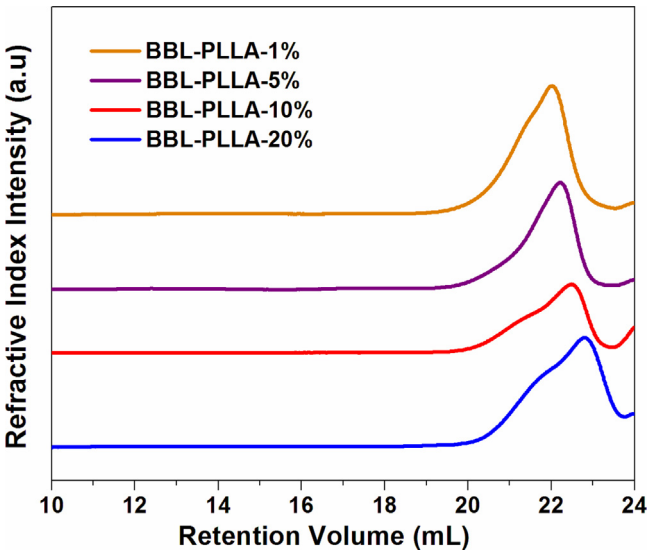

Fig. 2. GPC traces of BBL-*g*-PLLA graft copolymers.

by controlling the side chain length of PLLA. It was found that the conversion of LLA determined by ^{1}H NMR (Fig. 1) was high in the each BBL-*g*-PLLA copolymer (>80%). Quantitative information about molecular weight and molecular weight distribution of copolymers were obtained using gel permeation chromatography (GPC). The M_n of BBL-*g*-PLLA copolymers could be controlled from 2544–7033 g mol^{-1} by manipulating the BBL content from 1.0 to 20 wt.% in the polymerization process (see Table 2 for details). It was difficult to measure the molecular weight of BBL-PLLA-40% by GPC due to poor solubility in THF [29]. The GPC traces of BBL-*g*-PLLA copolymers are shown in Fig. 2. It was worth mentioning that these traces were found to be narrow and monomodal, which indicated that the obtained purified copolymers were pure graft copolymers [30]. Furthermore, the PDI of the BBL-*g*-PLLA copolymers were relatively low according to the data of GPC (Table 2), implying that the preparation of BBL-*g*-PLLA copolymers via ROP could be well controlled using TBD as the catalyst [31]. BBL-*g*-PLLA copolymer (Table 2, BBL-PLLA-5%) was used for characterization of properties described in the later sections of this study.

3.3. Investigation of the dissolution behavior of BBL-g-PLLA copolymer

In this work, it was found that the solubility of BBL could be greatly improved in dichloromethane after PLLA grafting. The suitable BBL-*g*-PLLA copolymer was added to dichloromethane, stirred for 5 min and obtained the stability of the resulting dissolution (Fig. 3(1a)). Additionally, the process of BBL was as same as that of BBL-*g*-PLLA (Fig. 3(1b)). The BBL-*g*-PLLA solution still exhibited good dissolution characteristic after 24 h (Fig. 3(2a)), but it was clearly observed that BBL was precipitated in the bottom of bottle (Fig. 3(2a)). Thus, grafting by LLA could change the properties of the BBL. In the next section, the successful attachment of the PLLA side chains onto BBL backbone was confirmed with FT-IR, NMR and UV–vis techniques respectively.

3.4. Verification of BBL-g-PLLA copolymer

Fig. 4a shows that the FT-IR spectrum of BBL-*g*-PLLA copolymer. According to the IR spectrum, a novel absorption peak appeared at 1747 cm^{-1} compared with the BBL [12], which could be assigned to the stretching frequency of the carboxyl band of PLLA side chains, and the peaks observed at 3000 cm^{-1} and 2950 cm^{-1} were

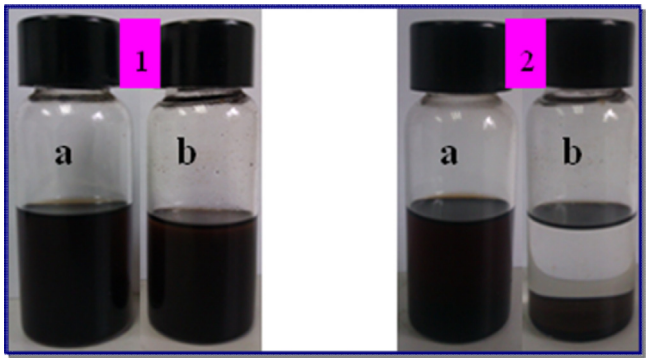

Fig. 3. Photographs of the dissolution of BBL-*g*-PLLA (a) and BBL (b) in dichloromethane: pictures recorded (1) 5 min stirred treatment and (2) 24 h later.

attributed to the characteristic absorbance of methyl and methylene groups in PLLA respectively. Details concerning the BBL-*g*-PLLA copolymer structure information were obtained using ^{1}H NMR and ^{13}C NMR characterization. A typical ^{1}H NMR spectrum of the graft copolymer BBL-*g*-PLLA with the assignment is presented in Fig. 4b. The major resonance peaks (a, 5.29 ppm; b, 1.57 ppm) had been assigned to PLLA. But it was worth mentioning that the proton signal (a′, 4.35 ppm) was ascribed to the terminal methylene of PLLA segments [30]. Fig. 4c shows a typical ^{13}C NMR spectrum and the assignment for PLLA segments. The expected peaks assigned to PLLA (173.7 ppm (a), 69.5 ppm (b) and 16.7 ppm (c)) could be obviously observed. The signal at 173.7 ppm was assigned to the carbonyl group, which was in good agreement with the aforementioned FTIR data. It could be seen that there was only one peak for the carbonyl of PLLA, indicating that BBL-*g*-PLLA were pure graft copolymers, which was in accordance with the aforementioned GPC data. It was noted that the BBL signals for the graft copolymers were difficult to be observed in the NMR spectra (including ^{1}H NMR and ^{13}C NMR), which was maybe because a low mass content BBL was presenting in copolymer [24]. However, UV–vis spectroscopy had been rather useful in further confirming the existence of the BBL in copolymers. The results are shown in Fig. 4(d). Compared with the pure PLLA, UV–vis absorption spectra of BBL and BBL-*g*-PLLA were similar, displaying the characteristic absorption band of aromatic rings at around 277 nm attributed to the BBL [32]. From the above results obtained, it could be concluded that the BBL-*g*-PLLA copolymer was successfully prepared.

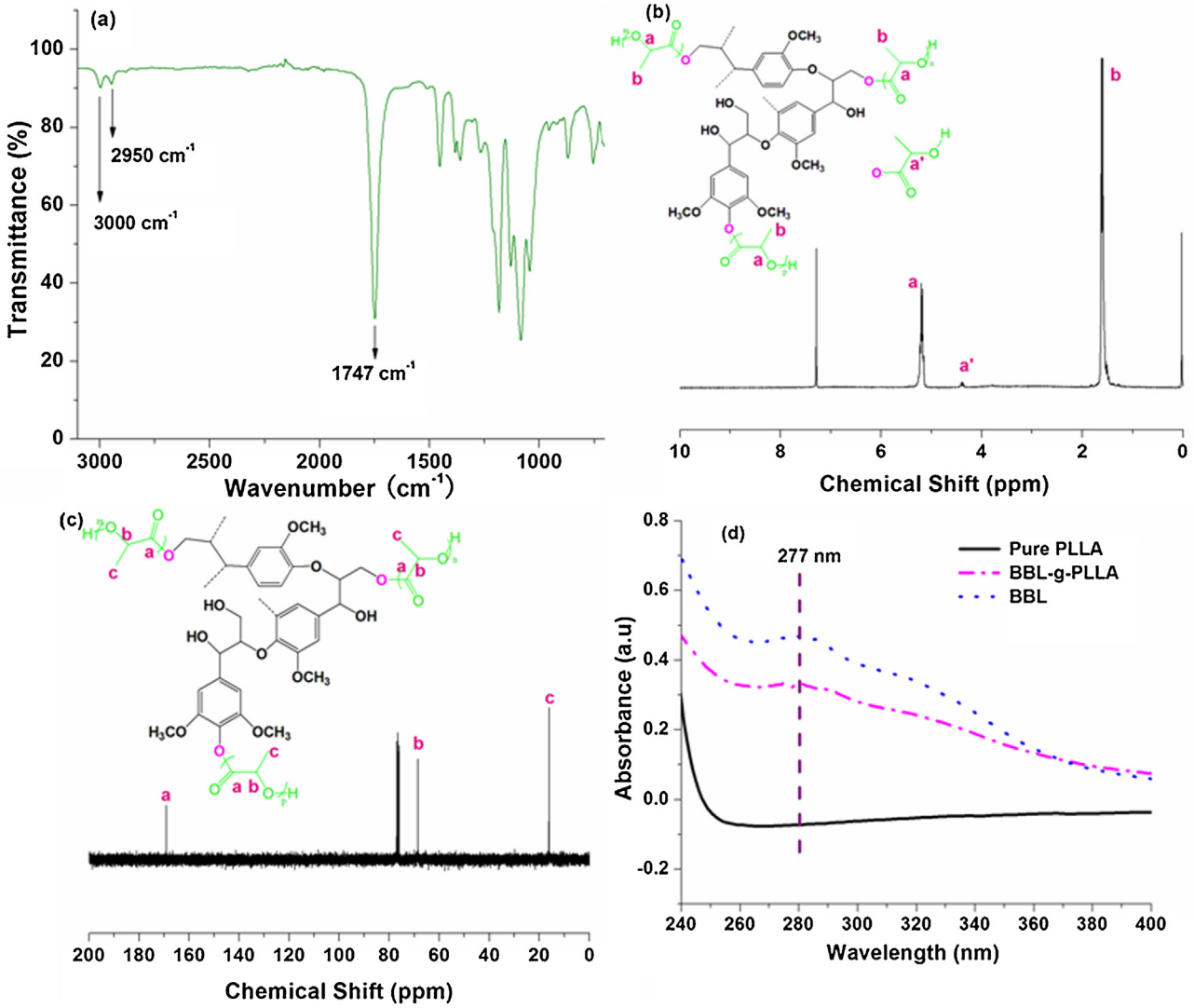

Fig. 4. (a) FTIR spectrum of BBL-*g*-PLLA copolymer, (b) ^{1}H NMR spectrum of BBL-*g*-PLLA copolymer ($CDCl_3$), (c) ^{13}C NMR spectrum of BBL-*g*-PLLA copolymer ($CDCl_3$) and (d) UV absorption spectra of BBL, BBL-*g*-PLLA and pure PLLA.

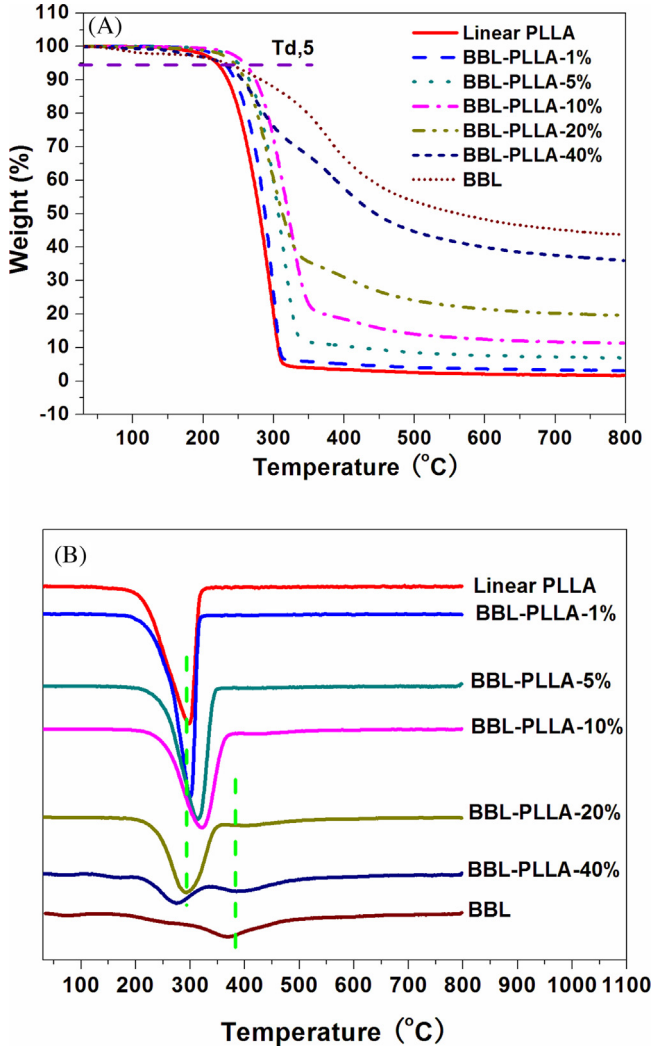

Fig. 5. (A) TGA and (B) DTG thermograms of BBL, linear PLLA and BBL-*g*-PLLA copolymers.

Table 3
Thermal properties of linear PLLA, BBL and BBL-*g*-PLLA graft copolymers.

Sample	$T_{d,\ 5}$ [°C][a]	$T_{d,\ max}$ [°C][b]	Char residue [wt.%][c]
Linear PLLA	219	297	1.68
BBL[d]	238	362	45.9
BBL-PLLA-1%	230	300	3.1
BBL-PLLA-5%	250	314	7.0
BBL-PLLA-10%	258	322	11.3
BBL-PLLA-20%	244	292, 402	19.7
BBL-PLLA-40%	228	274, 384	36.1

[a] $T_{d,\ 5}$ is 5 wt.% decomposition temperature.
[b] $T_{d,\ max}$ is the temperature corresponding to the maximum rate of weight loss.
[c] Obtained by TGA curves at 800 °C.
[d] The data was from Liu et al. [10].

3.5. Thermal properties of BBL-g-PLLA graft copolymers

We investigated the thermal stability of the copolymer, which was one of the most significant factors when it was considered being put into practice [33]. The thermal stability and decomposition behavior of BBL, BBL-*g*-PLLA copolymers and linear PLLA were characterized by thermogravimetric analysis (TGA) technique. The TGA and DTG are illustrated in Fig. 5(A, B). The relevant data (including $T_{d,5}$, $T_{d,\ max}$ and char residue) obtained from TGA and DTG are presented in Table 3. It was clearly observed that BBL and linear PLLA exhibited single peak for the maximum degradation rate at 362 and 297 °C, respectively. It was noted that the $T_{d,\ 5}$ and $T_{d,\ max}$ values of BBL-*g*-PLLA copolymers were lower than those of the BBL, indicating that the attachment of PLLA onto BBL led to a decrease in the thermal stability. This was because that the PLLA suffered from poor thermal stability. It should also be mentioned that the BBL-*g*-PLLA copolymers displayed a single mass loss step degradation profile with a low BBL content (1–10%). At a higher BBL content (20–40 wt.%), the decomposition of BBL-*g*-PLLA copolymer sample had two stages (e.g., BBL-PLLA-40% copolymer). The temperature of the first weight loss was about 274 °C and the second plateau was around at 384 °C. The $T_{d,\ max}$ for the first stage (274 °C) was very closely to that of linear PLLA (297 °C), indicating that this stage was attributed to the cleavage of part of the PLLA side chains, and the second stage (384 °C) was assigned to the cleavage of part of BBL backbone (362 °C). Additionally, the star-like BBL-*g*-PLLA copolymers showed higher $T_{d,\ max}$ than that of linear PLLA, which was possible associated with the effect of architectures. The star structure restricted the chain mobility of BBL-*g*-PLLA copolymer, which delayed the onset of catastrophic decomposition [34]. Meanwhile, it was found that the char residue of BBL-*g*-PLLA copolymers were higher than that of linear PLLA, and the char residue increased with an increase in BBL loading because of the high content of aromatic components in BBL [16].

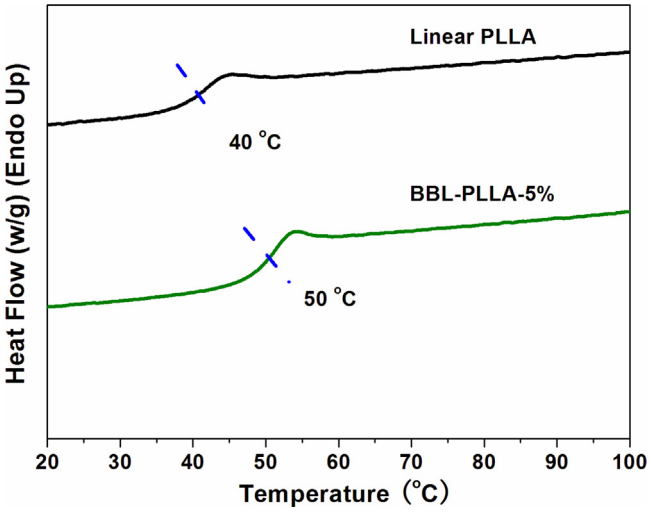

Fig. 6. DSC curves of linear PLLA and BBL-*g*-PLLA copolymers.

Lignin was a rigid and hyperbranched macromolecule and it was essential to investigate the influence of introducing BBL onto PLLA segments. Fig. 6 shows the DSC exothermic curves of linear PLLA and BBL-*g*-PLLA copolymers. As compared to the T_g value of the linear PLLA (40 °C), BBL-*g*-PLLA graft copolymer displayed a higher value of T_g at 50 °C could be attributed to the incorporation of the rigid and bulky BBL in the PLLA structure, resulting in hindering chain mobility of PLLA segments. According to the DSC analysis, the copolymers possessed a higher transition temperature. The similar result was reported in the literature [22]. It further indicated that T_g of BBL-*g*-PLLA copolymers was tunable.

3.6. Surface characterization of BBL substrate grafted with PLLA

Contact angle measurements were used to estimate the change in hydrophobicity of the grafted substrates compared to unmodified BBL, and a distinct difference in hydrophobicity was observed. The results were shown in Fig. 7. The contact angle of the coating film of the BBL was measured to be 73° (±5) (Fig. 7a), while that of the BBL-*g*-PLLA coating film obtained from BBL-*g*-PLLA

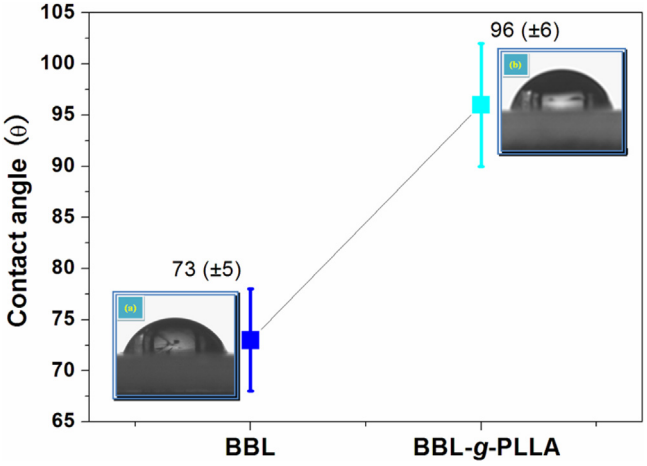

Fig. 7. Water contact angles of (a) BBL film (73° (±5)) and (b) BBL-*g*-PLLA copolymer film (96° (±6)) on glass surface. Each result was an average of five measurements.

copolymer was 96° (±6) (Fig. 7b), suggesting that the hydrophobicity of LLA was successfully grafted onto BBL. But it was found that the contact angle value of BBL-*g*-PLLA was higher in comparison to the values of pure PLLA found in the literature. This was maybe because contact angles were highly dependent on the sample preparation and the measurement method [35]. Furthermore, the value of PCL-grafted BBL coating film in our previous study [13] was lower than that of PLLA-grafted BBL coating film. This was possibly due to a more hydrophobic character of PLLA as compared to PCL [36].

Field-emission scanning electron microscopy (FE-SEM) was used to study the changes in surface morphology after grafting. Fig. 8 shows a lager difference in the structure of BBL compared to the PLLA-grafted BBL. It was clearly seen that BBL exhibited an irregular and rough surface with different sizes of agglomerates and blocks (Fig. 8a), which was in good agreement with literatures [37,38]. After PLLA grafting, the morphology of BBL-*g*-PLLA copolymer was changed to relatively smooth surface (Fig. 8b), indicating that the surface had been covered with PLLA layer.

In order to investigate how well the PLLA grafts cover BBL surface, X-ray photoelectron spectroscopy (XPS) measurements were performed. XPS was a powerful tool for surface analysis to investigate the changes in the elemental composition and structure groups of BBL and BBL-*g*-PLLA copolymer. Analysis of the XPS wide scan spectrum of BBL-*g*-PLLA revealed a peak at C 1s at 284.6 eV and a characteristic peak O 1s at 533 eV (Fig. 9A). In comparison with the oxygen of BBL (21.64 wt.%), the formation of the BBL-*g*-PLLA resulted in a remarkable enhancement of the oxygen signal (35.62 wt.%). Fig. 9B shows low resolution spectrum of BBL-*g*-PLLA. The C 1s signals were resolved into three components peaks (289 eV: O—C=O or 286.6 eV: C—O, and C—O—C or 284.6 eV:

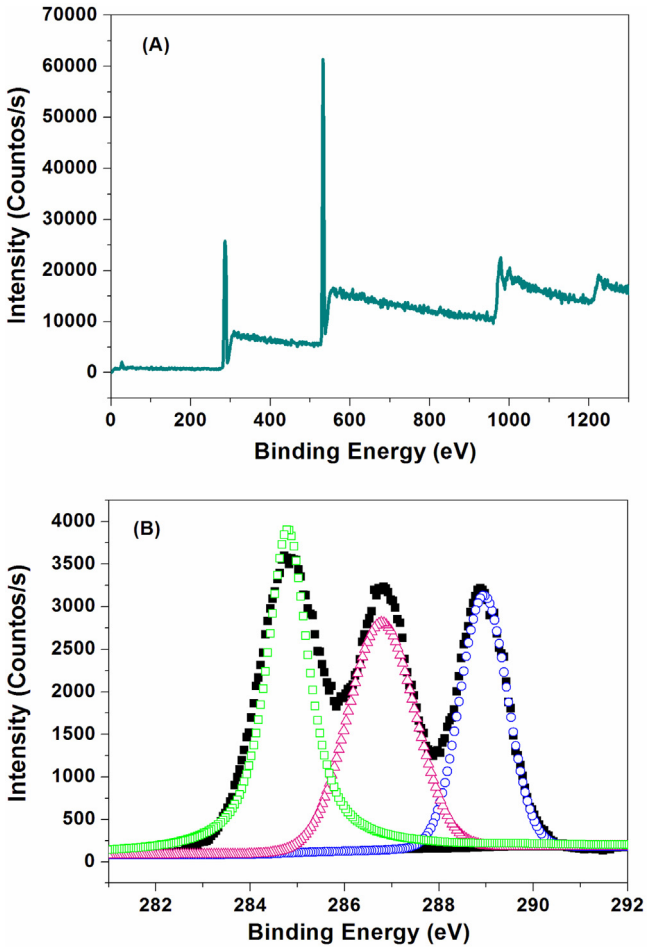

Fig. 9. XPS wide scan (A) and high-resolution carbon spectrum (B) from BBL-*g*-PLLA copolymer.

C—H, C—C, and C=C) [16]. The relative proportions of three oxidation levels of BBL and BBL-*g*-PLLA are calculated and presented in Table 4. It was found that the O—C=O groups content of BBL-*g*-PLLA (36.83 wt.%) was increased in comparison to that of BBL (6.14 wt.%). Moreover, the C—O groups content of BBL-*g*-PLLA (31.52 wt.%) was increased compared with that of BBL (23.20 wt.%). It was worth mentioning that the experimental mass ratios of C/O of BBL-*g*-PLLA (1.81) was close to the theoretical value obtained by the PLLA (1.13), confirming that the surface of BBL-*g*-PLLA coating film was covered with PLLA segments. The above conclusions could explain the fact that hydrophobicity of BBL coating film was increased as a result of PLLA grafting.

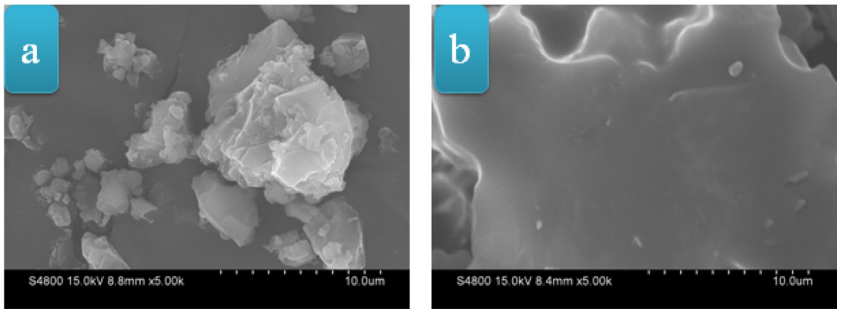

Fig. 8. FE-SEM microphotographs of BBL at (a) 5000×, and BBL-*g*-PLLA at (b) 5000×.

Table 4
Fraction of carbon functional groups from high resolution C1s XPS peaks.

	Surface elemental composition [wt.%]			Surface chemical groups [wt.%]		
	C	O	C/O	O—C=O	C—O	C—C
Sample				289(eV)	286.6(eV)	284.6(eV)
BBL[a]	78.36	21.64	3.62	6.14	23.20	70.66
BBL-PLLA-5%	64.38	35.62	1.81	36.83	31.52	31.64
PLLA (theoretical)	–	–	1.13	–	–	–

[a] The data was from Liu et al. [12].

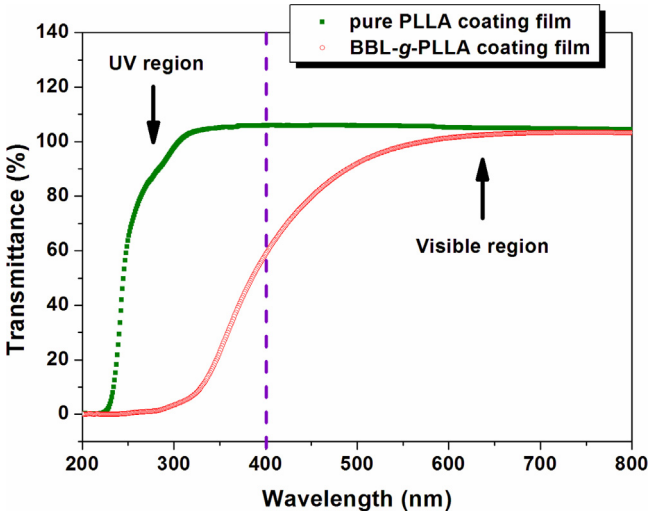

Fig. 10. UV-visible transmittance curves of pure PLLA and BBL-*g*-PLLA coating films on the quartz glass.

3.7. Investigation of the optical properties of BBL-g-PLLA coating films

UV–vis spectroscopy had been rather useful in testing the UV absorption properties [39]. Thus, pure PLLA and BBL-*g*-PLLA copolymer coating films were to investigate the light barrier property by UV–vis measurement. Fig. 10 shows the optical transmittance spectra within the UV–visible regions (200–800 nm) on the films obtained from pure PLLA and BBL-*g*-PLLA copolymer. It was worth noting that the transmittance of BBL-*g*-PLLA coating film dropped dramatically from 58% to 0% in the region ranging from 400 to 280 nm, while the transmittance of pure PLLA coating film slightly was reduced from by 100–95%. This was due to the introduction of BBL. The results obtained were in good agreement with reports in the literature [34]. Meanwhile, the wavelength at coating of BBL-*g*-PLLA exhibited transmittance of over 90% was found to be 500 nm. Based on the above results obtained, it could be concluded that BBL-*g*-PLLA copolymer could be expected to serve as a UV-absorbent film [22,40].

4. Conclusions

In summary, a graft copolymer, lignin-*graft*-poly (L-lactide) (BBL-*g*-PLLA), was synthesized by ROP of LLA at 135 °C in the presence of a triazabicyclodecene (TBD) catalyst under solvent-free. A series of BBL-*g*-PLLA copolymers with tunable number-average molecular weight (M_n) (2544–7033 g mol^{-1}) were obtained by manipulating the mass ratio of BBL/LLA and characterized by FT-IR, ^{1}H NMR, ^{13}C NMR, UV–vis, GPC, TGA, DSC, XPS, and FE-SEM spectroscopies. The BBL-*g*-PLLA graft copolymer displayed a higher value of T_g at 50 °C could be attributed to the incorporation of the rigid and bulky BBL in the PLLA structure. In comparison with BBL, BBL-*g*-PLLA copolymers showed poor thermal stability due to PLLA grafting. Moreover, with the increase of the BBL segments in the copolymer, the increase of char residue occurred. FE-SEM was used to study the change in surface morphology because of grafting. A relatively smooth surface was obtained after grafting, implying that the surface had been covered with PLLA segments. XPS analysis revealed that the hydrophobicity of LLA was successfully imparted into BBL, particularly on the surface. Furthermore, the UV absorption tests showed a UV absorption capability of the BBL-*g*-PLLA coating film. This work was to fully utilize lignocellulosic butanol residue as the raw material to produce the biopolymer which could be considered as a UV-absorbent film.

Acknowledgements

E.M.Z acknowledges the financial support from the Special Fund for the Key Research Foundation of Taizhou University with Grant No. 2014PY027 and the Ecology Key Disciplines of Zhejiang Province in Taizhou University. X.H.L acknowledges the financial support from the Program for key Science and Technology Team of Zhejiang Province with Grant No. 2013TD17 and Scientific Research Foundation of Zhejiang Agriculture & Forestry University with Grant No. 2014FR070. S.Y.F acknowledges the financial support from the Program for Zhejiang Provincial Natural Science Foundation of China under Grant No. LZ16C160001. Y.Z.X acknowledges the financial support from the Study Program for Outstanding Scholars from Home and Abroad under Grant No. CAFYBB2011007.

References

[1] D.M. Alonso, J.Q. Bond, J.A. Dumesic, Catalytic conversion of biomass to biofuels, Green Chem. 12 (2010) 1493–1513.
[2] F.G. Calvo-Flores, J.A. Dobado, Lignin as renewable raw material, ChemSusChem 3 (2010) 1227–1235.
[3] O. Gordobil, R. Delucis, I. Egüés, J. Labidi, Kraft lignin as filler in PLA to improve ductility and thermal properties, Ind. Crops Prod. 72 (2015) 46–53.
[4] A.A. Morandim-Giannetti, J.A.M. Agnelli, B.Z. Lanças, R. Magnabosco, S.A. Casarin, S.H. Bettini, Lignin as additive in polypropylene/coir composites: Thermal, mechanical and morphological properties, Carbohydr. Polym. 87 (2012) 2563–2568.
[5] W.O. Doherty, P. Mousavioun, C.M. Fellows, Value-adding to cellulosic ethanol: lignin polymers, Ind. Crops Prod. 33 (2011) 259–276.
[6] M.P. Pandey, Lignin depolymerization and conversion: a review of thermochemical methods, Chem. Eng. Technol. 34 (2011) 29–41.
[7] M.N. Satheesh Kumar, A.K. Mohanty, L. Erickson, M. Misra, Lignin and its applications with polymers, J. Biobased Mater. Biol. 3 (2009) 1–24.
[8] Y.-S. Jang, A. Malaviya, C. Cho, J. Lee, S.Y. Lee, Butanol production from renewable biomass by clostridia, Bioresour. Technol. 123 (2012) 653–663.
[9] W. Zhang, Y. Ma, C. Wang, S. Li, M. Zhang, F. Chu, Preparation and properties of lignin–phenol–formaldehyde resins based on different biorefinery residues of agricultural biomass, Ind. Crops Prod. 43 (2013) 326–333.
[10] X. Liu, J. Wang, S. Li, X. Zhuang, Y. Xu, C. Wang, F. Chu, Preparation and properties of UV-absorbent lignin graft copolymer films from lignocellulosic butanol residue, Ind. Crops Prod. 52 (2014) 633–641.
[11] X. Liu, J. Wang, J. Yu, M. Zhang, C. Wang, Y. Xu, F. Chu, Preparation and characterization of lignin based macromonomer and its copolymers with butyl methacrylate, Int. J. Biol. Macromol. 60 (2013) 309–315.
[12] X. Liu, Y. Xu, J. Yu, S. Li, J. Wang, C. Wang, F. Chu, Integration of lignin and acrylic monomers towards grafted copolymers by free radical polymerization, Int. J. Biol. Macromol. 67 (2014) 483–489.
[13] X. Liu, E. Zong, J. Jiang, S. Fu, J. Wang, B. Xu, W. Li, X. Lin, Y. Xu, C. Wang, Preparation and characterization of Lignin-graft-poly (ε-caprolactone) copolymers based on lignocellulosic butanol residue, Int. J. Biol. Macromol. 81 (2015) 521–529.

[14] W.G. Glasser, R.K. Jain, Lignin derivatives. I. Alkanoates, Holzforschung 47 (1993) 225–233.
[15] W. Thielemans, R.P. Wool, Lignin esters for use in unsaturated thermosets: lignin modification and solubility modeling, Biomacromolecules 6 (2005) 1895–1905.
[16] J. Wang, K. Yao, A.L. Korich, S. Li, S. Ma, H.J. Ploehn, P.M. Iovine, C. Wang, F. Chu, C. Tang, Combining renewable gum rosin and lignin: towards hydrophobic polymer composites by controlled polymerization, J. Polym. Sci. A 49 (2011) 3728–3738.
[17] Y.S. Kim, J.F. Kadla, Preparation of a thermoresponsive lignin-based biomaterial through atom transfer radical polymerization, Biomacromolecules 11 (2010) 981–988.
[18] A. Hufendiek, V. Trouillet, M.A.R. Meier, C. Barner-Kowollik, Temperature responsive cellulose-graft-copolymers via cellulose functionalization in an ionic liquid and RAFT polymerization, Biomacromolecules 15 (2014) 2563–2572.
[19] D. Roy, M. Semsarilar, J.T. Guthrie, S. Perrier, Cellulose modification by polymer grafting: a review, Chem. Soc. Rev. 38 (2009) 2046–2064.
[20] A. Duval, M. Lawoko, A review on lignin-based polymeric, micro- and nano-structured materials, React. Funct. Polym. 85 (2014) 78–96.
[21] X. Zhang, M. Chen, C. Liu, A. Zhang, R. Sun, Homogeneous ring opening graft polymerization of ε-caprolactone onto xylan in dual polar aprotic solvents, Carbohydr. Polym. 117 (2015) 701–709.
[22] Y.-L. Chung, J.V. Olsson, Li R.J, C.W. Frank, R.M. Waymouth, S.L. Billington, E.S. Sattely, A renewable lignin–lactide copolymer and application in biobased composites, ACS Sustain, Chem. Eng. 1 (2013) 1231–1238.
[23] W. de Oliveira, W.G. Glasser, Multiphase materials with lignin 11. Starlike copolymers with caprolactone, Macromolecules 27 (1994) 5–11.
[24] S. Laurichesse, L. Avérous, Synthesis, thermal properties, rheological and mechanical behaviors of lignins-grafted-poly(ε-caprolactone), Polymer 54 (2013) 3882–3890.
[25] R.C. Pratt, B.G. Lohmeijer, D.A. Long, R.M. Waymouth, J.L. Hedrick, Triazabicyclodecene: a simple bifunctional organocatalyst for acyl transferand ring-opening polymerization of cyclic esters, J. Am. Chem. Soc. 128 (2006) 4556–4557.
[26] R. Todd, S. Tempelaar, G. LoRe, S. Spinella, S.A. McCallum, R.A. Gross, J.-M. Raquez, P. Dubois, Poly(ε-pentadecalactone)-b-poly(L-lactide) block copolymers via organic-catalyzed ring opening polymerization and potential applications, ACS Macro. Lett. 4 (2015) 408–411.
[27] Q.-F. Lü, Z.-K. Huang, B. Liu, X. Cheng, Preparation and heavy metal ions biosorption of graft copolymers from enzymatic hydrolysis lignin and amino acids, Bioresour. Technol. 104 (2012) 111–118.
[28] J. Lora, W. Glasser, Recent industrial applications of lignin: a sustainable alternative to nonrenewable materials, J. Polym. Environ. 10 (2002) 39–48.
[29] T. Saito, R.H. Brown, M.A. Hunt, D.L. Pickel, J.M. Pickel, J.M. Messman, F.S. Baker, M. Keller, A.K. Naskar, Turning renewable resources into value-added polymer: development of lignin-based thermoplastic, Green Chem. 14 (2012) 3295–3303.
[30] W. Yuan, J. Yuan, F. Zhang, X. Xie, Syntheses, characterization, and in vitro degradation of ethyl cellulose-graft-poly(ε-caprolactone)-block-poly(L-lactide) copolymers by sequential ring-opening polymerization, Biomacromolecules 8 (2007) 1101–1108.
[31] W. Yuan, J. Yuan, L. Zhou, S. Wu, X. Hong, Fe3O4@poly(2-hydroxyethyl methacrylate)-graft-poly(ε-caprolactone) magnetic nanoparticles with branched brush polymeric shell, Polymer 51 (2010) 2540–2547.
[32] H. Ohnishi, M. Matsumura, H. Tsubomura, M. Iwasaki, Bleaching of lignin solution by a photocatalyzed reaction on semiconductor photocatalysts, Ind. Eng. Chem. Res. 28 (1989) 719–724.
[33] J. Deng, B. Yang, C. Chen, J. Liang, Renewable eugenol-based polymeric oil-absorbent microspheres: preparation and oil absorption ability, ACS sustain, Chem. Eng. 3 (2015) 599–605.
[34] J. Yu, J. Wang, C. Wang, Y. Liu, Y. Xu, C. Tang, F. Chu, UV-absorbent lignin-based multi-arm star thermoplastic elastomers, Macromol. Rapid Commun. 36 (2015) 398–404.
[35] E. Schwach, L. Averous, Starch-based biodegradable blends: morphology and interface properties, Polym. Int. 53 (2004) 2115–2124.
[36] H. Lönnberg, Q. Zhou, H. Brumer, T.T. Teeri, E. Malmström, A. Hult, Grafting of cellulose fibers with poly(ε-caprolactone) and poly(L-lactic acid) via ring-opening polymerization, Biomacromolecules 7 (2006) 2178–2185.
[37] H. Li, Q. Zhang, P. Gao, L. Wang, Preparation and characterization of graft copolymer from dealkaline lignin and styrene, J. Appl. Polym. Sci. 132 (2015) 41900–41909.
[38] D.-z Ye, C. Jiang, L. Liu, X. Zhang, Graft polymers of eucalyptus lignosulfonate calcium with acrylic acid: Synthesis and characterization, Carbohydr. Polym. 89 (2012) 876–882.
[39] A. Hambardzumyan, L. Foulon, B. Chabbert, V.r. Aguieí-Beíghin, Natural Organic UV-Absorbent Coatings Based on Cellulose and Lignin: Designed Effects on Spectroscopic Properties, Biomacromolecules 13 (2012) 4081–4088.
[40] S. Jairam, R. Bucklin, M. Correll, et al., UV resistance of polystyrene co-butyl acrylate (PSBA) encapsulated lignin–saponite nanohybrid composite film, Mater. Design 90 (2016) 151–156.